Article ID:1007-2985(2011)06-0065-04

Investigation of Plasma Inducing Static Air Flow *

LI Feng[1], SHANG Shou-tang[1,2], CHENG Ming[1,2], SUN Bai-gang[1],
GUO Rui-qing[1], ZHAO Er-lei[1], YANG Hui[1]
(1. School of Jet Propulsion, Beijing University of Aeronautics and Astronautics, Beijing 100191, China;
2. Aeroengine Institute of Shenyang, Shenyang 110015, China)

Abstract: In this paper, plasma inducing static air flow is investigated, in which the plasma is generated by a high-voltage RF (radio frequence) actuator and the affection of different plasma actuator excitation intensities, size and situation to the flow field are analyzed. The investigative results show that the plasma actuator can induce and accelerate the static air flow, the flow accelerative character of the plasma actuator is significant and can be used to control flow, such as drag-reduction and acceleration of the vehicle, flow separation control of the engine inlet, or thrust-vectoring control of engine exit flow.

Key words: plasma actuator; magnetofluid; electrofluid; flow control
CLC number: V235.113 **Document code**: A

1 Introduction

Plasma is an electrical neutral, highly ionized gas composed of ions, electrons, and neutral particles. The plasma flow can be controlled by the MHD (magnetohydrodynamics) or EHD (electrohydrodynamics)[1-2], so the plasma technology can be used to control flow separation of the engine inlet[3-4], accelerate the exiting flow of scramjet and accomplish thrust-vectoring control in aeroengine or scramjet[5-6]. Plasma technology is used widely in the AJAX (Russian Hypersonic Vehicle concept) plan of Russian[7-9] and the HVEPS (Hypersonic Vehicle Electric Power System program) plan of USA[10-12]. England, France and some other country also appear great interested in plasma flow control technology[13-15].

In this paper, an plasma inducing static air flow scheme based on the control of plasma flow is proposed. This scheme is to investigate the inducing capability of the plasma actuator in static air flow.

2 Mathematic and Physical Model

In this investigation, the CFD scheme is a finite volume method, where the conservation equations of the flow field are Navier-Stokes equations. Momentum term F and energy items q_v produced by the MHD are added in conservation equations to investigate the character of plasma actuator inducing static air flow by the simulant methods. In the flow field simulation, turbulence model is the standard two equations $k-$

* **Received date**: 2011-09-07
Foundation item: Aeronautical Science Key Foundation of China(2010ZB06009); Natural Science Foundation of China (50476005)
Biography: LI Feng(1966-), male, was born in Zixing County, Hunan Province, professor and director of doctor students at Peking University of Aeronautics and Astronautics; research areas are combustion experiment and simulation.

ε model, the second-order upwind scheme is used to discretize the inviscid components of the equation system. Boundary conditions are defined for velocity inlet, pressure outlet, and solid wall (no slip boundary). The basic equations are as follows.

(1) The continuity equations: $\frac{\partial \rho}{\partial t}+\nabla\cdot(\rho U)=0$.

(2) The momentum equations: $\frac{\partial}{\partial t}\rho U+\rho U\cdot\nabla U=-\nabla P+\mu\nabla^2 U+F$, where ρ is density, μ is effective viscosity coefficient, $U=\{u,v,w\}$, u,v,w are velocity of x,y,z direction, F is the Lorentz force, which can be expressed as $F=J\times B$, where J is electrohy density, B is magnetic intensity, $J=\frac{1}{\mu_m}\nabla\times B$, where μ_m is magnetic permeability.

The magnetic equations: $\frac{\partial B}{\partial t}-\nabla\times(U\times B)-\frac{1}{\sigma\mu_m}\nabla^2 B=0$, where σ is electrohy permeability.

(3) The turbulence equations: turbulence model is the standard two equations $k-\varepsilon$ model.

k equations: $\frac{\partial}{\partial t}(\rho k)+\rho(U\cdot\nabla)k=\nabla\cdot[(\mu+\frac{\mu_t}{Pr_k})\nabla k]+G-C_D\rho k^{3/2}/l-\varepsilon_{em}^k$, ε equations: $\frac{\partial}{\partial t}(\rho\varepsilon)+\rho(U\cdot\nabla)\varepsilon=\nabla\cdot[(\mu+\frac{\mu_t}{Pr_\varepsilon})\nabla\varepsilon]+\frac{\varepsilon}{k}(C_1G-C_2\rho\varepsilon)-\varepsilon_{em}^{\varepsilon}$, where G is the turbulent kinetic energy term based on velocity gradient, μ_t is turbulence viscosity coefficient, ε_{em}^k and $\varepsilon_{em}^{\varepsilon}$ are electromagnetic term, which can bewritten as $\varepsilon_{em}^k=C_3\sigma B_0^2 k$, $\varepsilon_{em}^z=C_4\sigma B_0^2\varepsilon$, where $\sigma_k=1.0$, $\sigma_\varepsilon=1.3$, $\sigma_\zeta=1.0$, $C_1=1.44$, $C_{1\varepsilon}=1.44$, $C_2=1.92$, $C_3=0.5$, $C_4=1.0$, $C_\mu=0.09$, $\mu_t=C_\mu\rho k^2/\varepsilon$, $Pr_k=1.0$, $Pr_\varepsilon=1.3$.

(4) The energy equations:

$$\rho c_p\frac{\partial T}{\partial t}+\rho c_p(U\cdot\nabla)T=\nabla\cdot[\lambda(1+\frac{\mu_t}{\mu Pr_t}Pr)\nabla T]+q_v, \tag{10}$$

where c_p is constant pressure specific heat capacity, λ is thermal conductivity, and q_v is heat source.

The momentum and energy items produced by the plasma are added to the flow field calculation through the UDF interface.

3 Simulation Results and Analysis

In the simulation, the size of the plasma generator models is 3×4 mm^2, and the excitation intensity is selected as Ⅰ: 3 kHz, 4 kV, Ⅱ: 6 kHz, 4 kV. Figure 1 is the plasma actuator scheme. Figure 2 is the PIV flow velocity vector tested by the University of Notre Dame. Figure 3 is the mesh scheme. Figure 4 is the velocity vector of actuator I. Figure 5 is the velocity cloud of actuator I and figure 6 is the velocity section of actuator I. Figure 7 is the velocity vector of actuator Ⅱ, figure 8 is the velocity cloud of actuator Ⅱ and figure 9 is the velocity section of actuator Ⅱ.

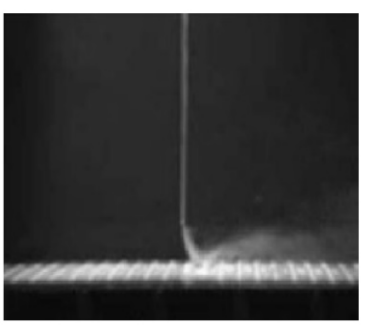

Figure 1 Plasma Actuators

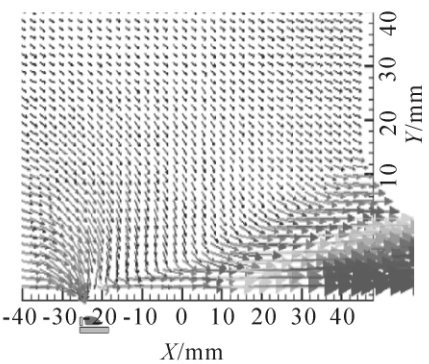

Figure 2 PIV Velocity Vector

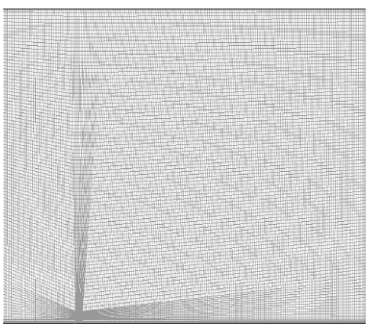

Figure 3 Mesh Scheme

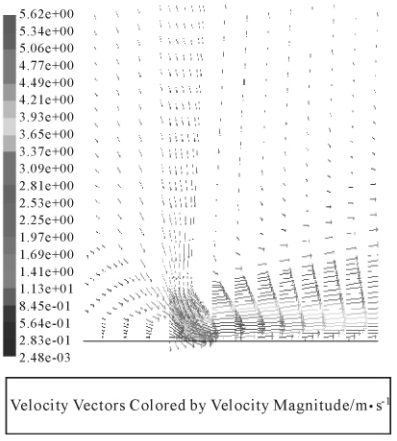

Figure 4　Actuator I Velocity Vector

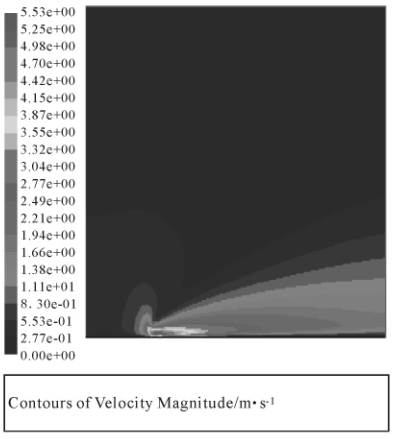

Figure 5　Actuator I Velocity Cloud

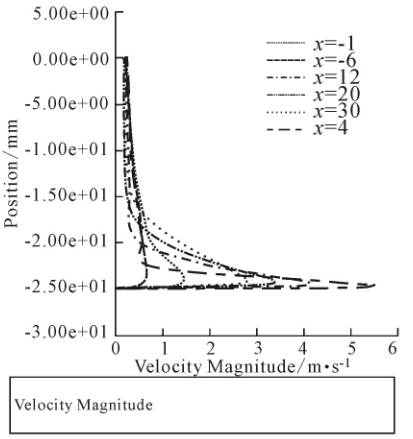

Figure 6　Actuator I Velocity Section

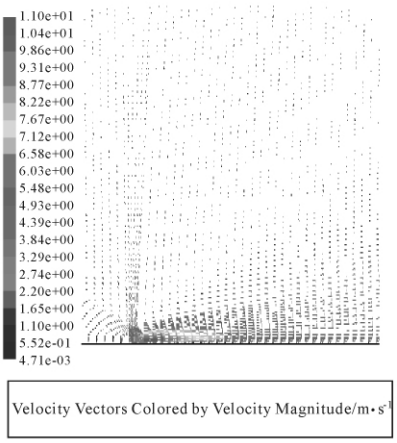

Figure 7　Actuator Ⅱ Velocity Vector

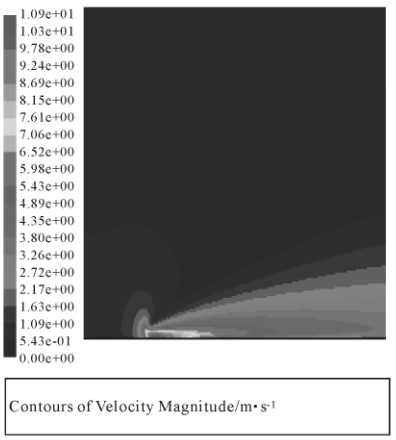

Figure 8　Actuator Ⅱ Velocity Cloud

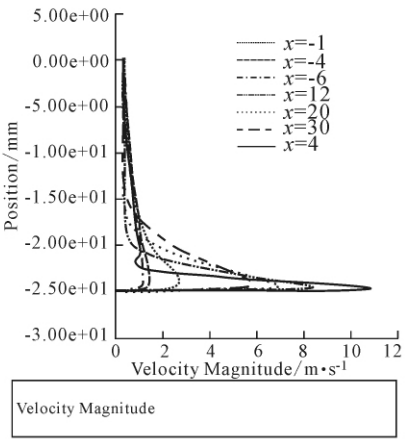

Figure 9　Actuator Ⅱ Velocity Section

From the experimental results of the University of Notre Dame at figure 2, we can find that the plasma generated under the conditions of high-voltage RF can affect the surrounding fluid.

By comparing the the simulant results at figure 4 and the experimental results at figure 2, we can find that the simulant velocity vector is very similar with the experimental velocity vector tested by the University of Notre Dame. So we can investigate the plasma inducing static air flow surrounding the actuator by the simulant methods in this paper.

From the simulant results as figure 5 and figure 6, the inducing velocity of actuator I is about 5m/s, the induce distance is about 25 mm, 10 times of the actuator size.

In figure 7, figure 8 and figure 9, We increase the excitation intensity 1 times as actuator Ⅱ, the induce velocity of actuator Ⅱ is about 10 m/s, higher than actuator I. The induce distance is about 25 mm, 10 times of the actuator size, without change.

4　Conclusion

The plasma inducing static air flow surrounding the actuator has been investigated in this paper, the follow conclusions can be drawn:

(1) the actuator can affect 10 times of the actuator size static air flow surrounding the actuator;

(2) excitation intensity increases, the inducing velocity of actuator increases, but the inducing distance is not changed;

(3) RF actuator can accelerate the flow field near the wall;

(4) increasing the voltage or the frequence of the RF actuator, we can increase the excitation intensi-

ty of the actuator and get higher induce speed.

The investigative results show that the plasma actuator can induce and accelerate the static air flow, the flow accelerative character of the plasma actuator is significant and can be used to control flow, such as flow separation control of the engine inlet, or thrust-vectoring control of engine exit flow.

References:

[1] BRUNO C, CZYSZ P A. Electro-Magnetic Interactions in a Hypersonic Propulsion System [C]. AIAA, 1997: 3 389.

[2] KUMAR R, HARIBALAN R. Hydrodynamic Model of Plasma-Sheath for RF Discharges with and Without Collision [C]. Reno, NV, USA: 43rd AIAA Aerospace Sciences Meeting and Exhibit, 2005: 948.

[3] SUZEN Y B. Numerical Simulation of Plasma Based Flow Control Application [C]. Toronto, Ontario, Canada: 35th AIAA Fluid Dynamics Conference and Exhibit, 2005: 4 633.

[4] SUBRATA R. Multidimensional Collisional Dielectric Barrier Discharge for Flow Separation Control at Atmospheric Pressure [C]. Capua, Italy: 13th AIAA International Space Planes and Hypersonics Systems and Technologies, 2005: 4 631.

[5] SERGEY B, LEONOV S. High-Speed Flow Control Due to Interaction with Electrical Discharges [C]. Capua, Italy: 13th AIAA International Space Planes and Hypersonics Systems and Technologies, 2005: 3 287.

[6] DAVID A, Minton R. Plasma and Magnetohydrodynamic Effects on Incipient Separation in a Cold Supersonic Flow [C]. Capua, Italy: 13th AIAA International Space Planes and Hypersonics Systems and Technologies, 2005: 3 224.

[7] CHASE R L, BOYD R, CZYSZ P, et al. An AJAX Technology Advanced SSTO Design Concept [C]. Reno, NV, USA: 36th AIAA Aerospace Sciences Meeting and Exhibit, 1998: 5 527.

[8] MARTIQUA L. Separation Flow Control Using plasma Actuators Dynamic Stall Control on an Oscilliating Airfoil [C]. Orlando, FL, USA: 1st AIAA Space Exploration Conference: Continuing the Voyage of Discovery, 2005: 2 517.

[9] THOMAS C. Application of Weakly-Ionized Plasmas as Wing Flow-Control Deverces [C]. Reno, NV: 40th AIAA Aerospace Sciences Meeting & Exhibit, 2002: 350.

[10] LINEBERRY J T, BEGG L, CASTRO J H, et al. Scramjet Driven MHD Power Demonstration-HVEPS Program [C]. San Francisco, California: 37th AIAA Plasmadynamics and Lasers Conference, 2006: 3 080.

[11] BOBASHEV S V. MHD Control of the Separation Phenomenon in a Supersonic Xenon Plasma Flow [C]. Reno, NV: 41st AIAA Aerospace Sciences Meeting & Exhibit, 2003: 1 068.

[12] HUANG J H. Plasma Actuators for Separation Flow Control of Low Pressure Turbine Blands [C]. Reno, NV: 41st AIAA Aerospace Sciences Meeting & Exhibit, 2003: 1 027.

[13] LEONOV S, BITYURIN V. The Features of Electro-Discharge Plasma Control of High-Speed Gas Flows [C]. Maui, HI: 33rd AIAA Plasmadynamics and Lasers Conference, 2002: 2 180.

[14] YAN R. Flow Visualization in a Supersonic Nonequilibrium Plasma Wind Tunnel [C]. Norfolk, VA: 30th AIAA Plasmadynamics and Lasers Conference, 1999: 3 725.

[15] SIDORENKO A. Plamsa Control of Separatted Flow Asymmetry on a Cone at High Angles of Attack [C]. Reno, NV: 42th AIAA Aerospace Sciences Meeting and Exhibit, 2004: 843.

等离子激励器对静止空气的诱导作用

李 锋[1], 尚守堂[1,2], 程 明[1,2], 孙佰刚[1], 郭瑞卿[1], 赵二雷[1], 杨 晖[1]

(1. 北京航空航天大学能源动力学院, 北京 100191; 2. 沈阳发动机设计所, 辽宁 沈阳 110015)

摘 要: 对等离子体发生器对静止空气诱导加速作用进行了数值模拟, 并与 Notre Dame 大学的相关实验结果进行了比较, 二者符合良好. 研究结果表明, 等离子体发生器对静止空气有诱导加速作用, 激励强度、等离子体发生器尺寸等对流体的诱导有较大影响. 该研究成果可用于飞行器的减阻增速、流动分离控制及推力矢量控制等.

关键词: 等离子体发生器; 磁流体; 电流体; 流动控制

中图分类号: V235.113 **文献标志码:** A (责任编辑 向阳洁)